

## Low-resistivity Au/Ni Ohmic contacts to Sb-doped *p*-type ZnO

L. J. Mandalapu, Z. Yang, and J. L. Liu<sup>a)</sup>

Quantum Structures Laboratory, Department of Electrical Engineering, University of California at Riverside, Riverside, California 92521

(Received 18 February 2007; accepted 29 May 2007; published online 18 June 2007)

Au/Ni contacts were fabricated on Sb-doped *p*-type ZnO film, which was grown on *n*-type Si (100) substrate with a thin undoped ZnO buffer layer by molecular beam epitaxy. As-deposited contacts were rectifying while Ohmic behavior was achieved after thermally annealing the contacts in nitrogen environment. Contact resistance was determined by linear transmission line method and it decreased with the increase of annealing temperature. Low specific contact resistivity of  $3.0 \times 10^{-4} \Omega \text{ cm}^2$  was obtained for sample annealed at 800 °C for 60 s. Secondary ion mass spectroscopy was used to analyze elemental profiles of the contacts before and after annealing. Zn vacancies created by outdiffusion of Zn are believed to couple with activated Sb atoms to increase the surface hole concentration enabling Ohmic contact formation. © 2007 American Institute of Physics. [DOI: 10.1063/1.2750400]

ZnO is a wide band gap semiconductor material that has drawn a lot of attention recently. However, *p*-type doping is extremely difficult due to the presence of native defects and donors.<sup>1-3</sup> Active research is currently carried out to explore various suitable *p*-type dopants for ZnO.<sup>4-10</sup> Recently, Sb-doped ZnO films grown on Si (100) substrates exhibited reliable and reproducible *p*-type behavior.<sup>7-10</sup> ZnO hetero- and homojunction devices were fabricated based on Sb-doped *p*-type ZnO films,<sup>11,12</sup> where Al/Ti metal was used for achieving Ohmic contacts to both *n*-type and *p*-type ZnO. However, relatively high contact resistance was observed for Al/Ti contacts on *p*-type ZnO, which limited our device performance. There are several reports on various metal schemes that have been employed for *p*-type ZnO films.<sup>13-17</sup> In this letter, we explore Au/Ni metal for making Ohmic contacts to Sb-doped *p*-type ZnO films.

Sb-doped ZnO films were grown on *n*-Si (100) substrates at 550 °C using a Perkin-Elmer molecular beam epitaxy system. Prior to growth, the Si substrates were cleaned by the piranha-HF method and dried by nitrogen, which was followed by thermal cleaning at 650 °C. A thin undoped ZnO buffer layer was grown to improve the crystalline quality of the subsequent Sb-doped ZnO layer. Undoped layer was grown for 30 min while the growth of Sb-doped layer was for 150 min, giving rise to an effective thickness of about 435 nm. Sb-doped ZnO layer was grown using Zn and Sb effusion cells. Oxygen plasma was generated by an electron-cyclotron-resonance source. A postgrowth annealing at 800 °C was carried out for 30 min to activate the acceptor dopants. Au/Ni bilayer metal of thickness 120/20 nm was deposited at room temperature. Rapid thermal annealing was performed at various temperatures of 700, 750, and 800 °C for 60 s in nitrogen environment to form Ohmic contacts. Room temperature Hall effect and resistivity measurements yielded a hole concentration, mobility, and resistivity of  $1 \times 10^{19} \text{ cm}^{-3}$ ,  $8 \text{ cm}^2 \text{ V}^{-1} \text{ s}^{-1}$ , and  $0.3 \Omega \text{ cm}$ , respectively, for the Sb-doped ZnO sample.

Transmission line patterns with size of  $75 \times 50 \mu\text{m}$  and with spacings of 10, 20, 30, and 40  $\mu\text{m}$  were fabricated by e-beam evaporation and lift-off. The fabricated patterns are shown as the inset of Fig. 1. Current-voltage (*I*-*V*) characteristics of these contacts were measured using 4155C parameter analyzer and Signatone probe station. The point of probing is shown by the arrows on a pair of contacts of the transmission line method (TLM) pattern. As-deposited contacts were found to be rectifying with very high contact resistance, as shown by the solid *I*-*V* curve in Fig. 1. The current conducted through them is of the order of nanoamperes. Figure 1 also shows the linear *I*-*V* characteristics indicating the establishment of Ohmic conduction for contacts that are annealed at 700 °C (dashed) and 800 °C (dotted). The contact resistance was found to decrease with the increase of annealing temperature, as seen from the increase in the magnitude of current. The total resistance, which includes contact resistance, was calculated from the slopes of *I*-*V* curves. A number of TLM patterns were measured and the total resistance with error factor was plotted as a function of the intercontact distance for all the annealed samples.

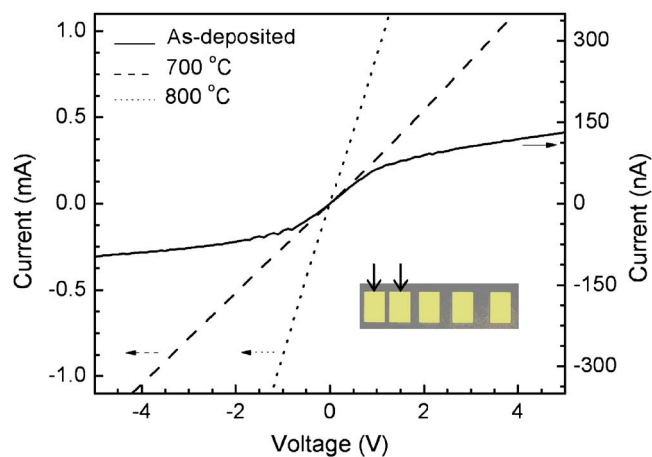


FIG. 1. (Color online) *I*-*V* characteristics of as-deposited contacts (solid line), annealed contacts at 700 °C (dashed line), and annealed at 800 °C (dotted line). The arrows show the point of probing on the schematic of the TLM patterns in the inset.

<sup>a)</sup> Author to whom correspondence should be addressed; electronic mail: jianlin@ee.ucr.edu

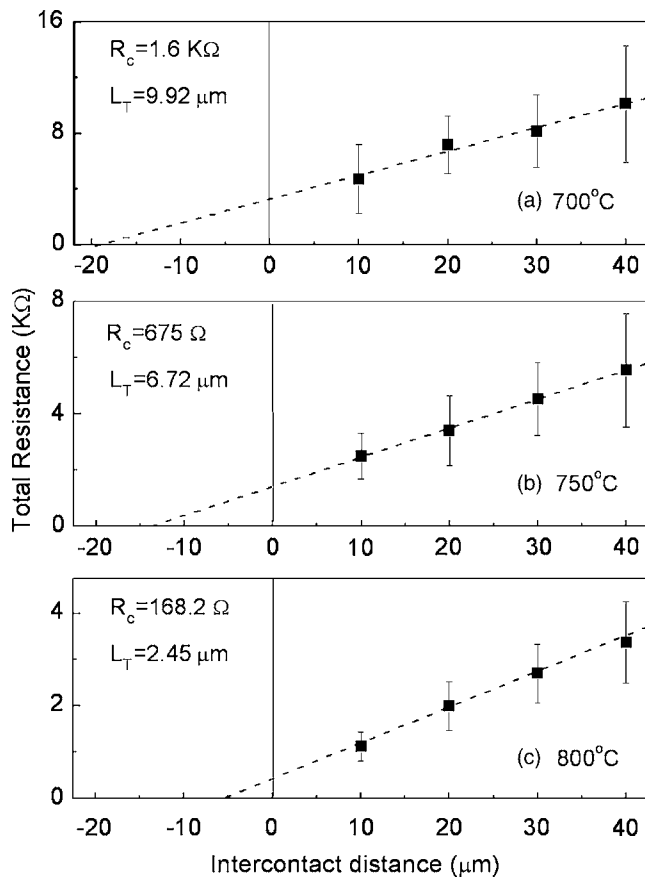


FIG. 2. Contact resistance as a function of intercontact distance for the samples annealed at (a) 700, (b) 750, and (c) 800 °C. The linear characteristics are extrapolated to obtain specific contact resistivity.

Figures 2(a)–2(c) show TLM result of the samples which were annealed at 700, 750, and 800 °C for 60 s. The linear characteristic was extrapolated to obtain the contact resistance and transfer length. For example, for the sample annealed at 800 °C, these values are of 168.2  $\Omega$  and 2.45  $\mu\text{m}$ , respectively. The specific contact resistivity of about  $3.0 \times 10^{-4} \text{ }\Omega \text{ cm}^2$  was then calculated.

The annealing temperature dependence of specific contact resistivity of samples is shown in Fig. 3. Although

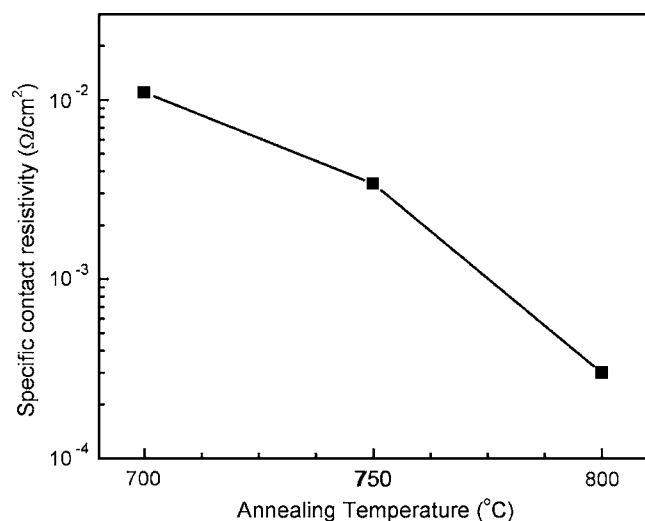


FIG. 3. Specific contact resistivity as a function of annealing temperature on a semilog plot. The lowest resistivity of  $3.0 \times 10^{-4} \text{ }\Omega \text{ cm}^2$  is obtained for the sample annealed at 800 °C.

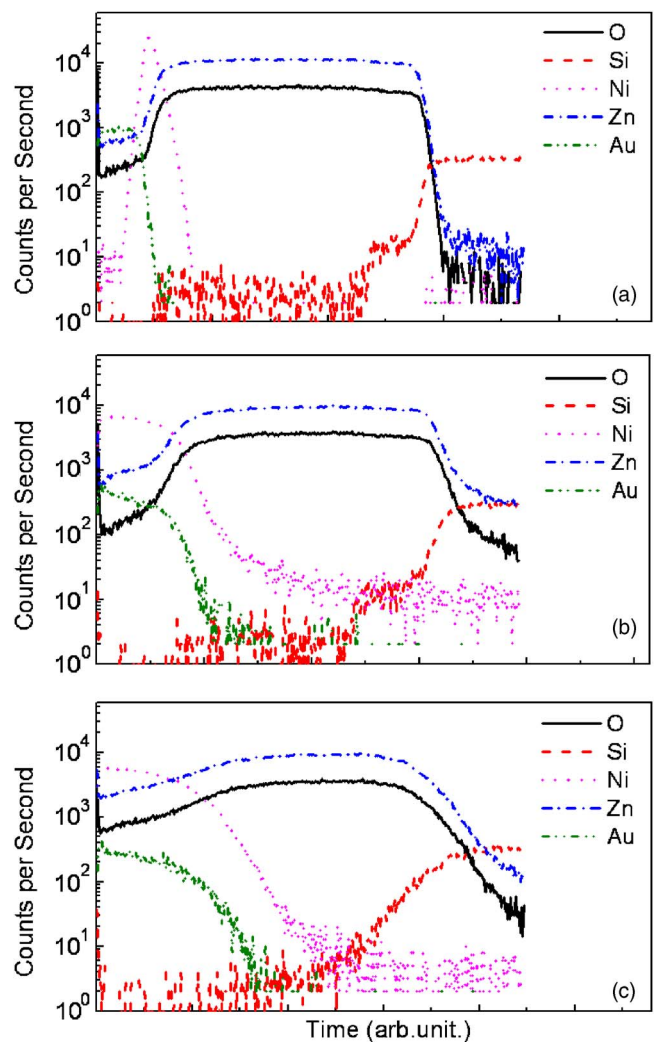


FIG. 4. (Color online) Elemental profiles of Au, Ni, Zn, O, and Si for samples with contacts (a) as deposited, (b) annealed at 700 °C, and (c) annealed at 800 °C.

Ohmic contacts were established at 700 °C, the specific contact resistivity of the sample was relatively high at about  $1.2 \times 10^{-2} \text{ }\Omega \text{ cm}^2$ . The specific contact resistivity decreases noticeably with increasing annealing temperature. The lowest value of  $3.0 \times 10^{-4} \text{ }\Omega \text{ cm}^2$  is obtained for the sample annealed at 800 °C, which is about two orders of magnitude lower than that for 700 °C. As a matter of fact, the values are comparable with the contact resistivities of the Ohmic contacts to phosphorus-doped *p*-type ZnO which are low enough for exploring efficient optoelectronic devices.<sup>13–15</sup>

To understand possible reason of Ohmic contact formation on Sb-doped *p*-type films, secondary ion mass spectroscopy (SIMS) measurements were carried out to obtain the Zn, O, Au, Ni, and Si elemental profiles of the samples before and after annealing. ZnO layer on Si substrate, thin layer of Ni, and thick layer of Au are clearly identified in Fig. 4(a) for the as-deposited sample. The profiles are distinct without noticeable interdiffusion between metal and ZnO. For the sample annealed at 700 °C, as shown in Fig. 4(b), interdiffusion of Zn, O with Ni, and Au can be observed. O at the surface has increased while Au has decreased slightly. This is due to the surface oxidation during thermal annealing. Outdiffusion of Zn is also observed, which may be responsible for the formation of Ohmic contacts. Outdiffusion of Zn cre-

ates Zn vacancies in the ZnO film.<sup>15</sup> Zn vacancies by themselves produce acceptor levels that are relatively deep. However, these vacancies can couple with activated Sb atoms to form  $\text{Sb}_{\text{Zn}}+2V_{\text{Zn}}$  and produce shallow acceptor levels.<sup>10,18</sup> This helps us to form low-resistance contacts as the depletion region of the Schottky diode becomes very thin due to strong *p*-type behavior and holes can tunnel through easily. The sample annealed at 800 °C, as shown in Fig. 4(c), confirms further outdiffusion of Zn, creating more Zn vacancies and hence, better contact resistivity through increased hole concentration.

In summary, Au/Ni Ohmic contacts to Sb-doped *p*-type ZnO film were achieved by rapid thermal annealing. The lowest specific contact resistivity of  $3.0 \times 10^{-4} \Omega \text{ cm}^2$  was obtained for the contacts annealed at 800 °C. The possible reason for the formation of Ohmic contacts involves an original high hole concentration of  $1 \times 10^{19} \text{ cm}^{-3}$  and the formation of additional Zn vacancies, which couple with activated Sb atoms to increase the local hole concentration. These results suggest that Au/Ni is a very good metal combination to form Ohmic contacts on Sb-doped *p*-type ZnO for optoelectronic device applications.

This work was supported by the DoD/DMEA through the center for NanoScience and Innovation for Defense (CNID) under Award No. H94003-06-2-0608 and the UCEI grant. The authors would like to acknowledge the SIMS measurements performed by Mikhail Klimov, Materials Characterization Facility, AMPAC, University of Central Florida.

- <sup>1</sup>U. Ozgur, Ya. I. Alivov, C. Liu, A. Teke, M. A. Reshchikov, S. Dogan, V. Avrutin, S. J. Cho, and H. Morkoc, *J. Appl. Phys.* **98**, 041301 (2005).
- <sup>2</sup>S. J. Pearton, D. P. Norton, K. Ip, and Y. W. Heo, *J. Vac. Sci. Technol. B* **22**, 932 (2004).
- <sup>3</sup>D. C. Look, *Mater. Sci. Eng., B* **80**, 383 (2001).
- <sup>4</sup>A. Tsukazaki, A. Ohtomo, T. Onuma, M. Ohtani, T. Makino, M. Sumiya, K. Ohtani, S. F. Chichibu, S. Fuke, Y. Segawa, H. Ohno, H. Koinuma, and M. Kawasaki, *Nat. Mater.* **4**, 42 (2005).
- <sup>5</sup>D. K. Hwang, H. S. Kim, J. H. Lim, J. Y. Oh, J. H. Yang, S. J. Park, K. K. Kim, D. C. Look, and Y. S. Park, *Appl. Phys. Lett.* **86**, 151917 (2005).
- <sup>6</sup>Y. R. Ryu, T. S. Lee, and H. W. White, *Appl. Phys. Lett.* **83**, 87 (2003).
- <sup>7</sup>F. X. Xiu, Z. Yang, L. J. Mandalapu, J. L. Liu, and W. P. Beyermann, *Appl. Phys. Lett.* **88**, 052106 (2006).
- <sup>8</sup>F. X. Xiu, Z. Yang, L. J. Mandalapu, and J. L. Liu, *Appl. Phys. Lett.* **88**, 152116 (2006).
- <sup>9</sup>F. X. Xiu, Z. Yang, L. J. Mandalapu, D. T. Zhao, J. L. Liu, and W. P. Beyermann, *Appl. Phys. Lett.* **87**, 152101 (2005).
- <sup>10</sup>F. X. Xiu, Z. Yang, L. J. Mandalapu, D. T. Zhao, and J. L. Liu, *Appl. Phys. Lett.* **87**, 252102 (2005).
- <sup>11</sup>L. J. Mandalapu, F. X. Xiu, Z. Yang, and J. L. Liu, *Appl. Phys. Lett.* **88**, 112108 (2006).
- <sup>12</sup>L. J. Mandalapu, Z. Yang, F. X. Xiu, and J. L. Liu, *Appl. Phys. Lett.* **88**, 092103 (2006).
- <sup>13</sup>J. H. Lim, K. K. Kim, D. K. Hwang, H. S. Kim, J. Y. Oh, and S. J. Park, *J. Electrochem. Soc.* **152**, G179 (2005).
- <sup>14</sup>S. Kim, B. S. Kang, F. Ren, Y. W. Heo, K. Ip, D. P. Norton, and S. J. Pearton, *Appl. Phys. Lett.* **84**, 1904 (2004).
- <sup>15</sup>H. S. Yang, Y. Li, D. P. Norton, K. Ip, S. J. Pearton, S. Jang, and F. Ren, *Appl. Phys. Lett.* **86**, 192103 (2005).
- <sup>16</sup>K. Ip, G. T. Thaler, H. Yang, S. Y. Han, Y. Li, D. P. Norton, S. J. Pearton, S. Jang, and F. Ren, *J. Cryst. Growth* **287**, 149 (2006).
- <sup>17</sup>S. H. Kang, D. K. Hwang, and S. J. Park, *Appl. Phys. Lett.* **86**, 211902 (2005).
- <sup>18</sup>S. Limpijumngong, S. B. Zhang, S. H. Wei, and C. H. Park, *Phys. Rev. Lett.* **92**, 155504 (2004).